Comparison of Hopfield Neural Network and Fuzzy Clustering in Segmenting Sputum Color Images for Lung Cancer Diagnosis

RACHID SAMMOUDA & FATMA TAHER
Department of Computer Science
University of Sharjah
P.O.B. 27272, Sharjah
UAE
rsammouda@sharjah.ac.ae, fatmat@sharjah.ac.ae
http://www.sharjah.ac.ae

Abstract: - The analysis of sputum taken from patients can be an extremely valuable technique for an early detection diagnosis of lung cancer. There is a great need for an automated system which can provide accurate analysis of the morphology of the sputum cells on a microscope slide, or diagnose their color digital image using special software. In this work, we compare two unsupervised segmentation methods of sputum color images, a modified Hopfield Neural Network (HNN), and a Fuzzy C-Mean (FCM) Clustering Algorithm. The segmentation results will be used as a base for a Computer Aided Diagnosis (CAD) system for early detection of lung cancer. Both methods are designed to classify the image of N pixels among M classes or regions. Due to intensity variations in background of the raw images, a pre-segmentation process is developed to standardize the segmentation process. In this study, we have used 1000 sputum color images to test both methods. Experimental evidence of the effectiveness and limitation of each method is reported.

Key-Words: - Hopfield Neural Network, Fuzzy Clustering, Segmentation, Sputum Color Images, Lung Cancer Diagnosis

1 Introduction

Lung cancer is considered to be as the leading cause of cancer death throughout the world and it is difficult to be at early stages, because symptoms appear only at advanced stages [1]. Physicians use several techniques to diagnose lung cancer, like chest radiograph and sputum cytological examination, where a sputum sample can be analyzed for the presence of cancerous cells [2]. However, the analysis process of the images obtained by this technique is still suffering from some limitation caused by the scanning process. Recently, some medical researchers have proven that the analysis of sputum cells can assist for a successful diagnosis of lung cancer. For this reason we attempt to come with an automatic diagnostic system for detecting lung cancer in its early stage based on the analysis of sputum color images. In this paper we present a new unsupervised segmentation algorithm to divide the image into several meaningful subregions as the first step in the image analysis process.

An index of the important role played by segmentation of color imagery in a great number of applications may be represented by the almost bewildering variety of techniques advanced to accomplish this task, such as histogram analysis, regional growth, edge detection and pixel classification. Good reference of these techniques can be found in [3]. Other authors have considered the use of color information as the key discriminate factor for cell segmentation for lung cancer diagnosis The analysis of sputum images had been used in [4] for detecting tuberculosis; it consists of analyzing sputum images for detecting bacilli.

In this paper, two basic segmentation techniques Hopfield Neural Network (HNN) and Fuzzy C-Mean Clustering Algorithm (FCM) are used to segment sputum color images prepared by the standard staining method described in [5]. In computer memory, each image is represented as three separate pixel matrices corresponding to their red, Green and blue intensity components in the RGB color space. The segmentation is performed to the regions of interest (ROI) extracted from the raw images based on a pre-segmentation process. We report a few segmentation results of both algorithms to compare their effectiveness.

2 Hopfield Neural Network

Hopfield neural network (HNN) is one of the artificial neural networks, which has been used in many papers in the literature for different

purposes, a good survey of the interesting features of HNN can be found in [6]. One of the related usages in medical image processing field is its use for classification of magnetic resonance (MR) images of the brain based on energy minimization as in [7-9]. All papers reported acceptable results. In [8], we have improved the algorithm used in [7] to overcome some of the problems reported by the authors of [7], such as considering the minimization of the sum of the errors squares, which can lead to better minimization than the simple sum of errors, and also, we ensured the convergence of the network in a pre-specified period of time.

Hopfield Neural Network (HNN) architecture consists of a grid of N x M neurons with each column representing a class and each row representing a pixel, N represents the size of the given image and M represents the number of classes that is given as a priori information. The network is designed to classify the feature space without teacher based on the compactness of each class calculated using a distance measure. The segmentation problem is formulated as a partition of N pixels of P features among M classes such that the assignment of the pixels minimizes the cost-term of the energy (error) function:

$$E = \frac{1}{2}\sum_{k=1}^{N}\sum_{l=1}^{M} R_{kl}^{n} V_{kl}^{2} \quad (1)$$

where Rkl is the Euclidian distance measure between the kth pixel and the centroid of class l, and is defined as follows:

$$R_{kl} = \left\| X_k - \overline{X}_l \right\| \quad (2)$$

where Xk is the feature vector of the kth pixel, and $\overline{X}_l$ is the centroid of class l, and defined as follows:

$$\overline{X}_l = \frac{\sum_{k=1}^{N} X_K V_{KL}}{n_l} \quad (3)$$

where nl is the number of pixels in class l.

In our case n=2 which means the energy is defined as sum of squared errors Vkl is the output of the klth neuron. We adopted the winner-takes-all learning rule, where the input-output function for the kth row (to assign a label m to the kth pixel) is given by:

$$\begin{cases} V_{kl}(t+1) = 1, if U_{kl} = Max\left[U_{kl}(t), \forall l\right] \\ V_{kl}(t+1) = 0, otherwise \end{cases} \quad (4)$$

The minimization is achieved by using HNN and by solving a set of motion equations satisfying:

$$\frac{\partial U_i}{\partial t} = -\mu(t)\frac{\partial E}{\partial V_i} \quad (5)$$

Where Ui and Vi are respectively the input and the output of the ith neuron, $\mu(t)$ is as defined in [8] a scalar positive function of time, which determines the length of the step to be taken in the direction of the vector $d = -\nabla E(V)$. The appropriate selection of the step $\mu(t)$ is some thing of an art, experimentation and a familiarity with a given class of optimization problems are often required to find the best function. In our case, by experiment, we found that the $\mu(t)$ function used in [8] for segmenting the MR data using HNN is also work fine for segmenting the CT data using the HNN:

$$\mu(t) = t * (T_s - t) \quad (6)$$

Where t is the iteration step and Ts is the pre-specified convergence time.

HNN algorithm for segmenting the extracted lung regions can be summarized in the following steps:

1. Initialize the input of neurons to random values.
2. Apply the input-output function (Vkl) defined above, to obtain the new output values for the each neuron, establishing the assignment of pixels to classes. The class member probabilities grow or diminish in a winner-takes-all style as a result of contention between classes. In winner-takes-all model, the neuron with the highest input value fires and takes a value 1, and all other neurons take the value 0.
3. Compute the centroid as defined above, for each class l.
4. Compute the energy function (E) as defined above,
5. Update the inputs Ukl using the following equation.

$$U_{kl}(t+1) = U_{kl}(t) + \frac{\partial U_i}{\partial t} \quad (7)$$

6. Repeat from step 2 until t = Ts. This process iteratively modifies the pixel label assignments to reach a near optimal final segmentation map.

3 Fuzzy Clustering

The problem of clustering can be stated as follows: Let $\{x_q : q = 1,.....,Q\}$ be a set of Q feature vectors, each feature vector $x_q = (x_q^1,.....,x_Q^N)$ has N components. The process of clustering is to assign the Q feature vectors into K clusters where each cluster is represented by its center C_k, $\{C_k : k = 1,.....K\}$ [10], the dimension of the feature vectors x_q and centers C_k is N.

Fuzzy Clustering has been used in many fields like pattern recognition and fuzzy identification [9]. A verity of fuzzy clustering methods has been proposed and most of them are based upon distance criteria. One problem with traditional clustering techniques is that there are only two values, either 1 or 0, to specify to what degree a data point belongs to a cluster, this problem can be solved by using fuzzy set methods. Therefore, fuzzy clustering solved the problem of overlaps between hard clusters and it has clear advantage over crisp and probabilistic clustering methods [10]. In fuzzy subsets, each pixel in an image has a degree to a cluster or a boundary, characterized by a membership value, so we can avoid making a crisp decision earlier and keep the information through the higher processing levels as much as possible [11].

Recently, there has been an increasing use of fuzzy logic theory for color image segmentation [12-17]. The most widely used algorithm is the Fuzzy C-Mean algorithm (FCM), it uses reciprocal distance to compute fuzzy weights. The FCM was introduced by J.C.Bezdek [17], this algorithm has as input a predefined number of clusters, which is must be given and c-means stands for an average location of all the members of particular cluster and the output is a partitioning of the clusters on a set of objects.

The FCM uses fuzzy weighting with positive weight {W} to determine the centroid {C} for k clusters. The weights minimize the constrained functional J, by using Euclidean distance, where

$$J(W_{qk}, c_k) = \sum_{(q=1,Q)} \sum_{(k=1,K)} (W_{qk,})^p \, \| x_q - c_k \|^2 \quad (8)$$

$$W_{qk} = (1/\| x_q - c_k \|^2) / \sum_{(k=1,K)} (1/\| x_q - c_k \|^2), \quad k = 1,..K, q = 1,...,Q \quad (9)$$

where W_{qk} is the weight for each input data, ck is the centroid for each cluster and p represents the fuzzy truth value and its data dependent.

The FCM allows each feature vector to belong to multiple clusters with various fuzzy membership values. Then the final classification will be according to the maximum weight of the feature vector over all clusters which is computed using equation 9 as reported in [10]. In our system the input data is representing by sputum color images, each image is 768x512 pixels, and each pixel is represented with its three components in the RGB color space, We use the FCM clustering algorithm to segment these images, and vary the number of clusters from three to six based on medical information, as it is explained in the next sections.

3.1 FCM Clustering Algorithm

Input: sputum color image as a set of vectors (each vector represents a pixel), where: $x_q = \{x_q^R, .x_q^G, x_q^B\}, q = 1,....,Q$, in the RGB color space and Q represents the total number of pixels in the input sputum color image.

k = number of clusters, Output: A set of k clusters.

Algorithm steps:

1. Initialize random weight for each pixel; it uses fuzzy weighting with positive weights $\{W_{qk}\}$ between [0, 1].

2. Standardize the initial weights for each q feature vector over all K clusters via:

$$W_{qk} = W_{qk} / \sum_{k=1,K} W_{qk} \quad (10)$$

3. Compute J from Equation 8, where p is equal 2, and in this case we get the desired result and if p increase beyond 2, the weightings tend to become more uniform, and this will affect the segmentation results.

4. Compute new centroids Ck, via

$$c_k = \sum_{(q=1,Q)} W_{qk} \mathrm{x}_q, k = 1,...,K \quad (11)$$

5. Update the weights {Wqk } via equation (9).

6. Assign each pixel to a cluster based on the maximum weight.

7. Compute the energy function (E) which is equal to:

$$E = \sum_{\mathrm{x}=1}^{N} \sum_{k=1}^{K} (\| x_q - c_k \|^2 O_{\mathrm{xk}}^2) \quad (12)$$

Where $\| x_q - c_k \|^2$ is the Euclidian distance which measures between the xth pixels and the centroid of class k, and Oxk is the fuzzy output of the xth pixels input.

8. Compute Jnew from Equation (8): If(|Jnew-Jold|< threshold value) then stop, else Jold = Jnew and go to step 2 above. The thresholding value is decided experimentally.

4 Segmentation Results

Here, we present the result obtained with two sample images, the first sample containing red cells surrounded by a lot of debris nuclei and a background reflecting a large number of intensity variation in its pixels values as shown in Figure1 (a). The second sample is composed of blue stained cells shown in Figure3 (a). Figure1 (b) and (c) show the segmentation result using HNN and the FCM, respectively, using the RGB components of the raw image shown in Figure1(a). As it is seen in the segmentation result of both algorithms (b) and (c) the nuclei of the cells were not detected, in case of HNN, and were not accurately represented in (c). For this reason we developed a mask to extract the regions of interest, described in [8], and the result is shown in Figure1 (d).

Figure1 (e) and (f) show the segmentation result using HNN and FCM, respectively, with the RGB components of the image in (d) and by fixing the clusters number to three. We realize that in case of HNN the nuclei of the cells are detected but not precisely, and in case of the FCM only part of the nuclei has been detected. We increased the clusters number to four as an attempt to solve the nuclei detection problem and the results obtained using HNN and the FCM are shown, respectively, in Figure1 (g) and (h).

Comparing the HNN segmentation result in (g) to the raw image in (d), we can say that the nuclei regions were detected perfectly, and also their corresponding cytoplasm regions. However, due to the problem of intensity variation in the raw image (d) and also due to the sensitivity of HNN, the cytoplasm regions were represented by two clusters. These cytoplasm clusters may be merged later if the difference in their mean values is not large.

Comparing the FCM segmentation result in (h) to the raw image (d), the nuclei regions are detected but they present a little of overlapping, the way that two different nuclei may be seen or considered as one nucleus, and this can affect the diagnosis results. The cytoplasm regions are smoother than in case of HNN, reflecting that the FCM is less sensitive to the intensity variation than HNN. A quantitative reflection of the above comparison and discussion is shown in Figure2, where it can be seen that the segmentation error at convergence is smaller with HNN than with the FCM. However the FCM is converging fifty iterations earlier than HNN.

Figure 3 (a) shows a sample of sputum color image stained with blue dye, Figure 3 (b) and (c) show its segmentation results by HNN and the FCM using its RGB. As it is seen in the segmentation results obtained by both algorithms in (b) and (c) the nuclei have not been detected and the background is represented by more than on color reflecting the intensity variation of the background in the raw image. A filter was needed to minimize the effect of the intensity variation as described in [8]. The result of this filter is shown in Figure 3 (d), where the background is set to one value or one color and the ROIs are left with their original color in the raw image. Figure 3 (e) and (f) are the segmentation results of the image in Figure3 (d) obtained using

HNN and FCM, respectively, with four clusters. Here, all the nuclei have been detected however a color cluster is missing in the result of the FCM Figure 3 (f). The same as mentioned in the pervious case of the red cells, HNN is more sensitive to intensity variation between nuclei-nuclei or nuclei-cytoplasm regions. This is clear in Figure 4 which shows quantitatively the energy function of HNN and FCM during the segmentation process of the blue sample.

4 Conclusion

We have presented two techniques, HNN and the FCM, for the segmentation of sputum color images. Both methods applied color information, conveniently embedded into two different energy functions formulating the segmentation problem and reflecting the amount or error committed when distributing pixels among clusters. Both algorithms went through an iteration process in order to minimize the values of their corresponding energy functions at convergence. We have reported some examples which confirm the good performance of both methods also we have discussed the advantages and limitations of each over the other. In our future work both results will be used as input to a Computer Aided Design (CAD) system for lung cancer diagnosis based on the shape analysis of the segmented cells.

References:

[1] The National Women's Health Information Center, U.S Department of Health and Human Services office on Women's Health, Lung Cancer, "http://www.4woman.gov/faq/lung.htm", 2003.

[2] F. Herb, HuilongGuan Culture, Lung cancer," http://www.4uherb.com/cancer/lung/about.htm", 2002.

[3] J. AbuHassam, "A Computer Aided Diagnosis Systems for Early Detection of Lung Cancer Based on the Analysis of Chest Computed Tomography CT Images," M.SC. Thesis, May, 2005.

[4] M.Forero-Vargas, E. L. Sierra-Ballen, J. Alvarez-Borrego, J. L P. Pacheco, G. Cristobal, L. Alcala, M. Desco, "Automatic Sputum Color Image Segmentation for Tuberculosis Diagnosis", in Proc. SPIE, pp. 251-261, 2001.

[5] R. Sammouda, N. Niki, H. Nishitani, S. Nakamura, and S. Mori, "Segmentation of Sputum Color Image for Lung Cancer Diagnosis," in Proc. Int. conf. on image processing, 1, pp. 243, 1997.

[6] H.Karim. Y. Zhang, "Hopfield Neural Networks—A Survey" Proceeding of the 6th WSEAS Int. Conf. on Artificial Intelligence, Knowledge Engineering and Data Bases, Corfu Island, Greece, February 16-19, 2007.

[7] S. C. Armatur, D. Piraino and Y. Takefuji, “Optimization neural networks for the segmentation of magnetic resonance images”, IEEE Transaction on Medical Imaging, vol. 11, no. 2, pp. 215-220, 1992.

[8] R. Sammouda, N. Niki, H. Nishitani, and E. Kyokage, "Segmentation of Sputum Color Image for Lung Cancer Diagnosis based on Neural Network", IEICE transaction on information and systems(8), 1998.

[9] Y. Li., P. Wen, D. Powers, and C. R. Clark, “LSB neural network based segmentation of MR brain images”, proceeding of the IEEE International conference on systems, Ma and Cybernetics, vol2. 2000.

[10] G. Castellano, A. M. Fanelli, M.A. Torsello, "Mining usage profiles from access data using fuzzy clustering " Proceeding of the 6th International Conference on Simulation, Modeling and Optimization, Lisbon, Portugal, Sept. 22-24, 2006.

[11] C. Looney, "A Fuzzy Clustering and Fuzzy Merging Algorithm," Technical Report, Computer Science, University of Nevada, Dec. 1999.

[12] H. Sun, S. Wang and Q. Jiang, "Fuzzy C-Mean based Model Selection Algorithms for Determining the Number of Clusters," Pattern Recognition, vol.37, pp.2027-2037, 2004.

[13] H. Cheng, X. Jiang, Y. Sun and J. Wang, "Color Image Segmentation: Advances and Prospects," Pattern Recognition, vol. 34, no. 12, pp. 2259-2281, 2001.

[14] Y. S. Chen, “An Efficient Fuzzy C-Means Clustering Algorithm for Image Data,” Mathematical Problems in Engineering and Aerospace Sciences, 2004.

[15] H. Cheng and X. Jiang, "Homogram Thresholding Approach to Color Image Segmentation," International conference on Computer Vision, Pattern Recognition and Image Processing, Atlantic City, 2000.

[16] A. Moghaddamzadeh and N.Bourbakis, "Segmentation of Color Image with Highlights and Shadows using Fuzzy Reasoning," Proceeding on SPIE Symposium, Electronic Imaging: Science and Technology, San Jose, Feb. 1995.

[17] J.C. Bezdek, "Fuzzy Mathematics in Pattern Classification," Ph.D. thesis, Center for Applied Mathematics, Cornell University, Ithica, N.Y., 1973.

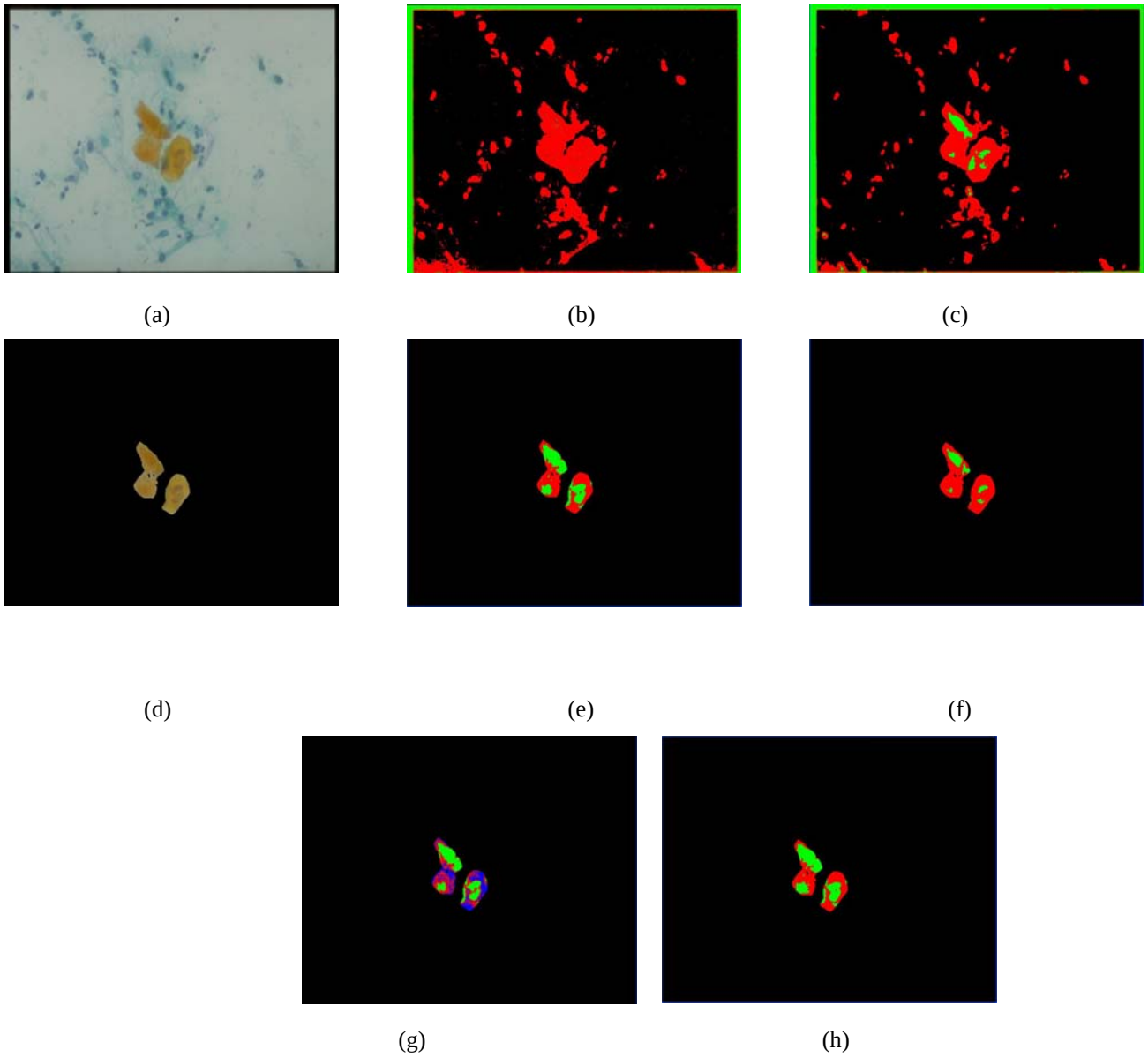

Figure 1. The image in (a) shows a sample of sputum color image stained with blue and red dyes. (b) and (c) show the segmentation result using HNN and the FCM with the RGB components of the raw image(a), respectively. (d) Shows the result of pre-segmentation masking process. (e) and (f) show the segmentation result using HNN and FCM with the RGB components of (d) and by fixing the clusters number to three, respectively, (g) and (h) are the results obtained by fixing the clusters number to four.

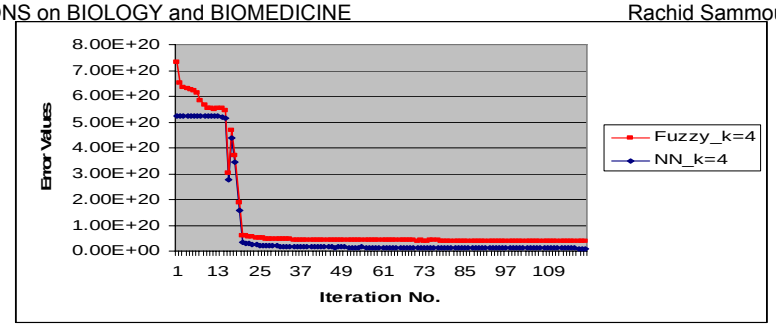

Figure 2. Shows the curves of the HNN and the FCM energy functions during the segmentation process of a sample of sputum color image stained with blue and dyes.

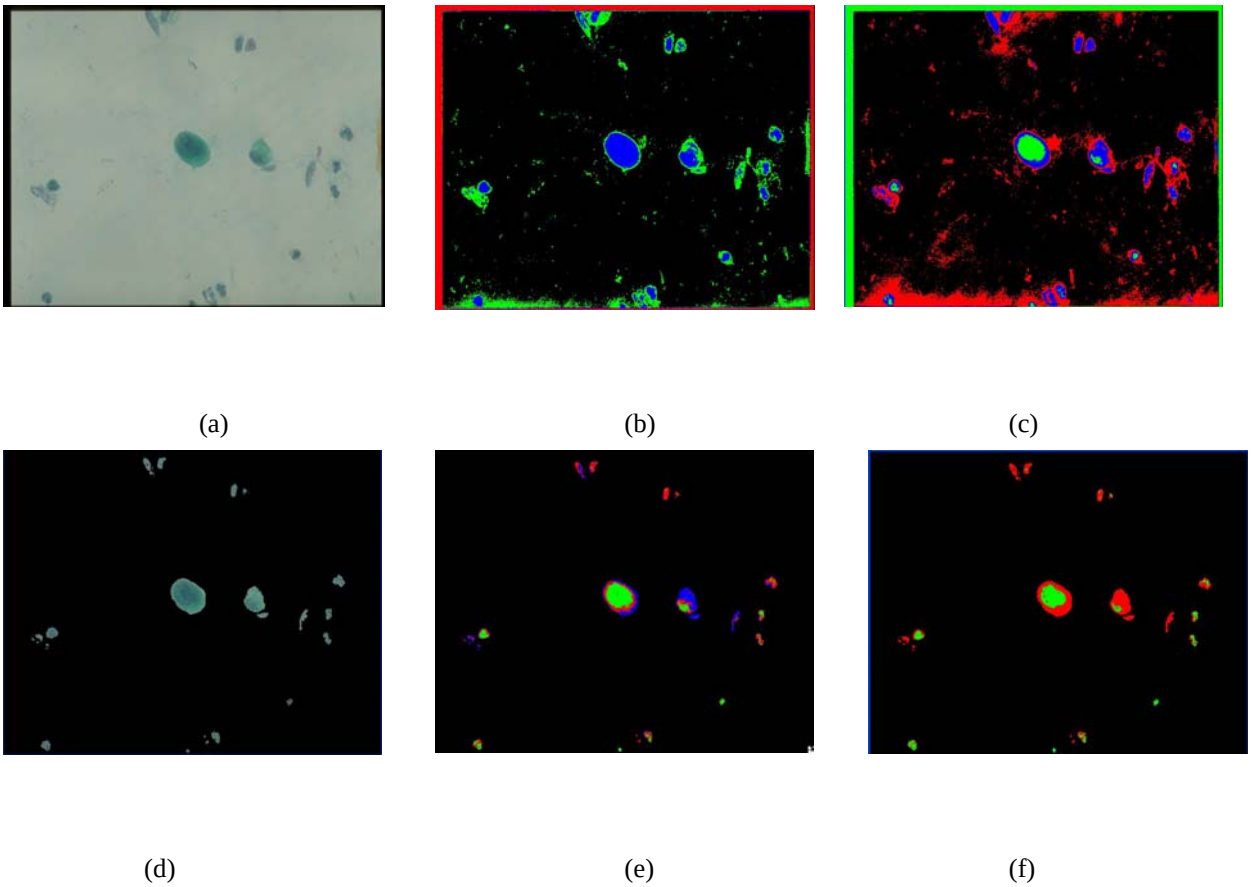

Figure 3. The image in (a) shows a sample of sputum color image stained with blue dyes. (b) and (c) show the segmentation result using HNN and the FCM with the RGB components of the raw image(a), respectively. (d) shows the result of pre-segmentation masking process. (e) and (f) show the segmentation result using HNN and FCM with the RGB components of (d) and by fixing the clusters number to four, respectively.

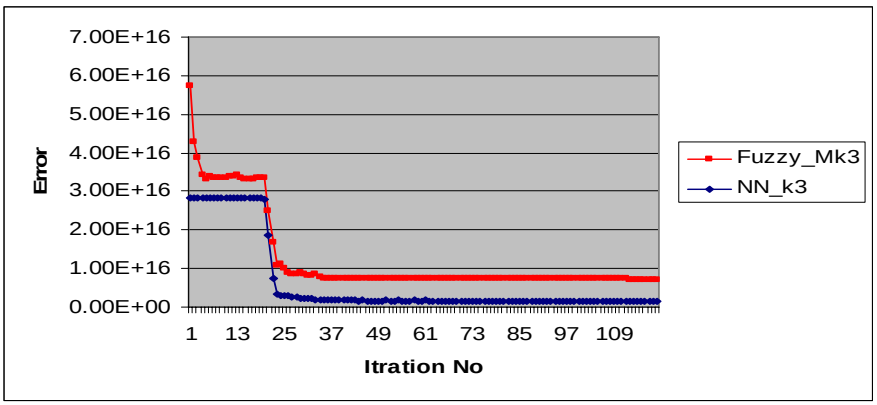

Figure 4. Shows the curves of HNN and the FCM energy functions during the segmentation process of a sample of sputum color image stained with blue dye.